In-Plane Ordering in Stage-2 Graphite Intercalation Compounds

doi: 10.1103/PhysRevB.27.3796

PHYSICAL REVIEW B VOLUME 27, NUMBER 6 15 MARCH 1983

In-plane ordering in stage-2 graphite intercalation compounds

C. Horie* and S. A. Solin
Department of Physics, Michigan State University, East Lansing, Michigan 48824

H. Miyazaki, S. Igarashi, and S. Hatakeyama
Department of Applied Physics, Tohoku University, Sendai, Japan
(Received 19 January 1982; revised mansucript received 30 July 1982)

A theoretical study of the orientational in-plane ordering in stage-2 graphite intercalation compounds is developed with particular emphasis on the role of phonons. Phonon dispersion curves are calculated within a simple phenomenological model. The rotation angle of intercalant layers relative to the graphite layers in the reciprocal-lattice space is shown to be determined predominantly by the transverse-acoustic mode. The rotation angles calculated for CsC_{24}, RbC_{24}, and KC_{24} are in fairly good agreement with experiments. The rotation angle depends also on the lattice constants of the host and guest layers. Our calculations have been carried out assuming a homogeneous triangular lattice structure for the intercalant layer. Comment is, therefore, made on the possibility of having a domain structure in which locally registered domains are bounded by discommensurations.

I. INTRODUCTION

It is well known by now that graphite intercalation compounds (GIC's) exhibit a wide variety of intraplanar and interplanar structural phase transitions when they are subjected to pressure and/or temperature variations.[1,2] Among the most intriguing of these transitions are those associated with in-plane orientational ordering in stage-2 alkali-metal GIC's.[1] For example, in CsC_{24} the intercalate layer exhibits positional disorder at $165 \leq T \leq 228$ K, but also shows an orientational epitaxy with the graphite host layer. The rotation angle associated with this epitaxy is temperature dependent through the above-mentioned range, but saturates to a temperature-independent value θ for $T \leq 165$ K. This saturation is associated with an in-plane ordering of the intercalate layer that has been ascribed a triangular lattice structure that is incommensurate with the graphite host.[3] More recently, it has been suggested that the intercalated layer orders into registered locally commensurate $(\sqrt{7}\times\sqrt{7})R19°$ and $(2\times2)R0°$ domains bounded by discommensurations.[4]

To date, few theoretical explanations of the above described phenomena have been provided. For CsC_{24} in the temperature range $165 \leq T \leq 228$ K the temperature dependence of θ is well accounted for phenomenologically by the Landau theory when it is applied to an orientational lock-in transition in which θ is the order parameter.[3] However, of greater interest is the dependence of the saturation value of θ on the species of alkali intercalant. Zabel[5] has attributed the variation of θ with intercalant to the lattice mismatch between host and guest layers. Clarke *et al.*[4] have attributed it to a species-dependent domain-size effect. Both of these explanations are inherently phenomenological and do not follow the role of phonons in the orientational transitions.

It may be expected that phonons play an important role in such transitions in GIC's because their role is crucial in the very similar orientational transitions exhibited by rare gases adsorbed onto grafoil, i.e., by materials that could be considered sister compounds of GIC's. Therefore, in this paper, we focus our attention on the orientationally ordered phase of CsC_{24} for $50 \leq T \leq 165$ K, but also consider RbC_{24} and KC_{24} and present a microscopic theory with particular emphasis on the role of phonons. The basic idea of the microscopic theory follows one developed by Novaco and McTague,[6] who studied the epitaxial ordering of monolayer films adsorbed on solid surfaces. We modify their theory so that it can be applied to the system consisting of intercalant layers sandwiched between a pair of graphite layers. It is shown that the total free energy consists of two terms, i.e., the mass-density-wave (MDW) energy E_{MDW} associated with an energy gain due to static displacement of atoms to their

most stable positions, and the free energy of phonons corresponding to vibrations of both intercalant atoms and carbon atoms around the stable positions. The relative orientation of a triangular lattice of an intercalant layer to a hexagonal carbon layer is described by the angle θ between $\vec{\tau}_{100}$ and $\vec{G}_{100}$, which are reciprocal-lattice vectors of the intercalant and graphite layers, respectively. The most stable orientation given by minimizing E_{MDW} with respect to θ is found at $\theta=14°$, 12°, and 8° for CsC_{24}, RbC_{24}, and KC_{24}, respectively, in good agreement with experiments.[3,7–9]

It is found that one of the most important factors which determine the rotation angle is the shape of the acoustic branches of the phonon dispersion curves at low frequencies. The in-plane vibrations of intercalant atoms are usually of low frequency and are coupled to the in-plane vibrations of carbon atoms, so that the dispersion curves of the acoustic-phonon modes of the compounds flatten noticeably at a very small wave vector and thus at low energy. This unusual feature of the dispersion curves of alkali-metal GIC's produces rotation angles which are significantly different from those observed in the epitaxial ordering of adsorbed rare-gas monolayers on graphite. The formulation of the MDW within a quasiharmonic phonon approximation is described in Sec. II. The phonon dispersion calculations are described in Sec. III for the case of CsC_{24}. Also in Sec. III the results of numerical calculations of the rotation angle are presented and compared with experiment. It is noted that if the magnitude $|\vec{\tau}_{100}|/|\vec{G}_{100}|$ is allowed to deviate from the ideal value corresponding to the in-plane stoichiometry of CsC_{24}, then the rotation angle changes correspondingly. In this connection, the possibility for an in-plane domain structure of intercalant layers is discussed. The conclusions are presented in Sec. IV.

II. MODEL OF ORIENTATIONAL ORDERING

Since we are interested in the orientational arrangement of intercalant layers relative to the graphite layers, we focus our attention only upon intercalant layers sandwiched between a pair of adjacent carbon layers, neglecting the interlayer interaction between intercalant layers, and we consider displacements of atoms parallel to basal planes. In our model, the dynamical motion of both intercalant and carbon atoms generates static MDW's that stabilize the orientationally ordered state. This is in contrast to the case of adsorbed rare-gas atoms, for which Novaco and McTague[6] have treated dynamical motions of adsorbed atoms under a static potential due to grafoil. Thus we extend the microscopic theory developed by Novaco and McTague[6] so as to be applicable to the present system.

We first consider the case of CsC_{24} and assume that the in-plane structure of an intercalant layer is a triangular lattice with a lattice constant d_I. The homogeneous intercalate layer requires the value of d_I to be fixed at 6.02 Å consistent with the in-plane stoichiometry of CsC_{24}. This value is also consistent with experimental observations.[3] Intercalant layers, therefore, are assumed to be nonregistered and incommensurate with adjacent hexagonal graphite layers that have a lattice constant $d_G=2.47$ Å.

We start with the Hamiltonian

$$H=H_I+H_G+H_{\mathrm{int}} , \tag{1}$$

where H_I and H_G represent the Hamiltonian of the subsystem of intercalant and graphite layers, respectively, and H_{int} represents the interaction between intercalant atoms and the neighboring carbon atoms (the interaction is assumed to be short ranged). Since we have neglected the interlayer interactions between intercalant layers, we can write H_I as follows:

$$H_I=\frac{\nu_I}{2M_I}\sum_j \vec{p}^{\,*}_{I,j}\cdot\vec{p}_{I,j} + \frac{\nu_I}{2}\sum_{i,j}\sum_{\vec{k}}\Phi^{II}_{\vec{k}}e^{i\vec{k}\cdot(\vec{R}^I_i-\vec{R}^I_j)}e^{i\vec{k}\cdot(\vec{u}^I_i-\vec{u}^I_j)} , \tag{2}$$

where ν_I is the number of intercalant layers, and the sum is carried out over atoms within the *same* layer. $\vec{R}^I_i$ is the lattice vector and $\vec{u}^I_i$ represents the displacement from $\vec{R}^I_i$. In the first approximation the dynamical motion of the intercalant atoms is considered to be determined by intercalant-intercalant atom force constants. Then, within the quasiharmonic approximation, the dynamical part of the Hamiltonian can be written as

$$H_I=\sum_{\vec{q},j}\hbar\omega_{I,j}(\vec{q})[a^\dagger_j(\vec{q})a_j(\vec{q})+\tfrac{1}{2}] , \tag{3}$$

where $a_j(\vec{q})$ and $a^\dagger_j(\vec{q})$ are annihilation and creation operators of the virtual phonon associated with dynamical motions of intercalant atoms around the lattice sites $\vec{R}^I_i$. Thus $\vec{u}^I_i$ is given by

$$\vec{u}^I_i=\frac{I}{\sqrt{N_I}}\sum_{\vec{q},j}\vec{e}_{I,j}(\vec{q})\left[\frac{\hbar}{2M_I\omega_{I,j}(\vec{q})}\right]^{1/2} \times e^{(i\vec{q}\cdot\vec{R}^I_j)}[a_j(\vec{q})+a^\dagger_j(-\vec{q})] , \tag{4}$$

where N_I is the number of lattice sites in the intercalant layers and $\vec{e}_{I,j}$ is the mode polarization.

We also introduce a set of operators $\{b_j(\vec{q}), b_j^\dagger(\vec{q})\}$ to describe virtual phonons associated with dynamical motions of carbon atoms in a similar approximation to that mentioned above. The motivation for introducing the dynamical motion of carbon atoms besides intercalant atoms is that (1) the phonon dispersion curves calculated for stage-1 GIC's (Ref. 10) demonstrate that the low-frequency motions of both intercalant and carbon atoms are strongly modulated with respect to each other; and (2) there is a transfer of electrons from intercalant alkali-metal atoms to the neighboring carbon atoms, giving rise to a screened Coulomb interaction between intercalant and carbon atoms. Usually the electrostatic interactions are considered to be much stronger than interactions between adsorbed rare-gas atoms and carbon atoms. Thus the total Hamiltonian can be written, omitting constant terms, as follows:

$$H=\sum_{\vec{q},l}\hbar\omega_{I,l}(\vec{q})[a_l^\dagger(\vec{q})a_l(\vec{q})+\tfrac{1}{2}]+\sum_{\vec{q},l}\hbar\omega_{G,l}(\vec{q})[b_l^\dagger(\vec{q})b_l(\vec{q})+\tfrac{1}{2}]$$
$$+\sum_{\vec{q},\vec{q}'}\sum_{l,l'}K_{\vec{q},\vec{q}',l,l'}[a_l^\dagger(-\vec{q})+a_l(\vec{q})][b_{l'}^\dagger(-\vec{q}')+b_{l'}(\vec{q}')]+\sum_{\vec{q},l}C_{\vec{q},l}[a_l^\dagger(-\vec{q})+a_l(\vec{q})]$$
$$+\sum_{\vec{q},l}D_{\vec{q},l}[b_l^\dagger(-\vec{q})+b_l(\vec{q})]\,, \tag{5}$$

where

$$K_{\vec{q},\vec{q}',l,l'}=\sum_{\vec{G}}\sum_{\vec{\tau}}\delta_{\vec{q}'-\vec{G},\vec{\tau}-\vec{q}}(N_IN_G)^{1/2}[\hbar^2/4M_IM_G\omega_{I,l}(\vec{q})\omega_{G,l'}(\vec{q}')]^{1/2}$$
$$\times[(\vec{\tau}-\vec{q})\cdot\vec{e}_{I,l}(\vec{q})][(\vec{q}'-\vec{G})\cdot\vec{e}_{G,l'}(\vec{q}')]U(\vec{\tau}-\vec{q})S(\vec{G})\,, \tag{6}$$

$$C_{\vec{q},l}=i\sum_{\vec{G}}\sum_{\vec{\tau}}\delta_{\vec{G}+\vec{q},\vec{\tau}}N_I^{1/2}N_G[\hbar/2M_I\omega_{I,l}(\vec{q})]^{1/2}[\vec{G}\cdot\vec{e}_{I,l}(\vec{q})]U(\vec{G})S(\vec{G})\,, \tag{7}$$

$$D_{\vec{q},l}=-i\sum_{\vec{G}}\sum_{\vec{\tau}}\delta_{\vec{G},\vec{\tau}+\vec{q}}N_IN_G^{1/2}[\hbar/2M_G\omega_{G,l}(\vec{q})]^{1/2}[\vec{\tau}\cdot\vec{e}_{G,l}(\vec{q})]U(\vec{\tau})S(\vec{G})\,. \tag{8}$$

The third term in Eq. (5) represents the dynamical coupling between two sets of virtual phonons associated with vibrations of intercalant atoms and carbon atoms, respectively. The function $U(\vec{q})$ in Eqs. (6)–(8) is the Fourier transform of the interaction potential between carbon and intercalant atoms. The summations $\sum_{\vec{G}}$ and $\sum_{\vec{\tau}}$ are over the reciprocal-lattice points of the hexagonal graphite layer and the triangular intercalant layer, respectively. Also $S(\vec{G})$ represents the two-dimensional (2D) structure factor of the hexagonal graphite layer.

The usual method to obtain a complete set of phonons is not applicable to the present case of incommensurability because there is no common finite unit cell. Moreover, the fact that there is no common finite Brillouin zone leads us to difficulties that we have to include interactions between all virtual phonons in the two systems of intercalant and carbon atoms and not their finite subsets. This would, of course, invalidate the usual procedure of diagonalization of the Hamiltonian. We need, therefore, to employ the following approximation to bring the Hamiltonian into a tractable form. First, we confine ourselves to the small Brillouin zone of the intercalant lattice and ignore interactions with phonons with wave vectors outside the Brillouin zone. Thus we consider interactions only between virtual phonons with $\vec{q}'=-\vec{q}'$ in the third term of Eq. (5). This approximation will not produce serious errors in the final result obtained below because $U(\vec{q})$ in Eq. (6) is important only for a sufficiently small $|\vec{q}|$. This point will be discussed in the next section. Second, in the present calculations described below, we take the six low-lying modes of virtual phonons polarized parallel to the basal plane of the crystal, because phonons with low frequencies are found to play an important role of stabilizing the MDW. Finally, an approximate but physically reasonable determination of $\omega_{I,j}(\vec{q})\omega_{G,j}(\vec{q})$ is made by referring to the phonon dispersion curves of KC_8. The details will be described in the next section.

The six virtual phonon modes that are considered

here are two acoustic modes, E_{2g} rigid layer shear modes, and two optical modes. By the analogy with the case of KC_8, the E_{2g} rigid layer modes and the two acoustic modes can be assigned as being associated with vibrations of carbon atoms so that they are described by $\{b_{l1}(\vec{q}),b_{l1}^{\dagger}(\vec{q})\}$ and $\{b_{l2}(\vec{q}),b_{l2}^{\dagger}(\vec{q})\}$, respectively, where $l=L,T$ denote the polarization. On the other hand, the optical modes associated with vibrations of intercalant atoms relative to carbon lattices are assigned as being intercalant virtual phonon modes and are described by $\{a_l(\vec{q}),a_l^{\dagger}(\vec{q})\}$ with $l=L,T$.

The two sets of virtual phonons are not exact phonons representing harmonic motions of all atoms around the most stable positions. In fact, those virtual phonons are modulated with respect to each other by means of the interatomic potential between intercalant and carbon atoms. The real phonons of the crystal are obtained by diagonalizing the Hamiltonian H. It is convenient to diagonalize H in two steps. First, we introduce a new set of operators $\{A_{l,m}(\vec{q}),A_{l,m}^{\dagger}(\vec{q})\}$, each of which is defined by a linear combination of $a_l(\vec{q})$, $a_l^{\dagger}(-\vec{q})$, $b_{l1}(\vec{q})$, $b_{l1}^{\dagger}(-\vec{q})$, $b_{l2}(\vec{q})$, and $b_{l2}^{\dagger}(-\vec{q})$ with the same polarization, and diagonalize the bilinear terms of H. This canonical transformation yields new frequencies $E_{l,m}(\vec{q})$ for the phonons. The number of independent modes with frequencies $E_{l,m}(\vec{q})$ is, of course, equal to the number of the relevant virtual phonon modes, and they are classified by the suffix m as well as l. Then the Hamiltonian is written as

$$H=\sum_{l,m}\sum_{\vec{q}}\{\hbar E_{l,m}(\vec{q})[A_{l,m}^{\dagger}(\vec{q})A_{l,m}(\vec{q})+\tfrac{1}{2}] +g_{l,m}(\vec{q})A_{l,m}(\vec{q}) +g_{l,m}^{*}(-\vec{q})A_{l,m}^{\dagger}(-\vec{q})\} . \quad (9)$$

The details of the canonical transformation yielding Eq. (9) are described in the Appendix. The frequencies $E_{l,m}(\vec{q})$ for the new phonons are given by the solutions of cubic equation (A5) and are specified by the polarization index l and the branch suffix $m=1$, 2, 3. The explicit expression for $E_{l,m}$ is not written here because it is lengthy and too complex. The explicit expression for $g_{l,m}(\vec{q})$ is given by Eq. (A8).

We introduce new phonon operators $\tilde{A}_{l,m}(\vec{q})$ and $\tilde{A}_{l,m}^{\dagger}(\vec{q})$ by the equations

$$A_{l,m}(\vec{q})=\tilde{A}_{l,m}(\vec{q})+\eta_{l,m}(\vec{q}) , \quad (10)$$

$$A_{l,m}^{\dagger}(\vec{q})=\tilde{A}_{l,m}^{\dagger}(\vec{q})+\eta_{l,m}^{*}(\vec{q}) , \quad (11)$$

where $\eta_{l,m}(\vec{q})$ and $\eta_{l,m}^{*}(\vec{q})$ are c-numbers determined by the conditions

$$\langle\tilde{A}_{l,m}(\vec{q})\rangle=\langle\tilde{A}_{l,m}^{\dagger}(\vec{q})\rangle=0 . \quad (12)$$

Here, the notation of angular brackets means the statistical average over the equilibrium state of new phonons. The conditions (12) guarantee that the new phonons described in terms of $\{\tilde{A}_{l,m}(\vec{q}),\tilde{A}_{l,m}^{\dagger}(\vec{q})\}$ represent harmonic motion of atoms around a stable arrangement of lattices, so that $\eta_{l,m}(\vec{q})$ and $\eta_{l,m}^{*}(\vec{q})$ are associated with the MDW's generated.[6] The average of the total energy is then given by

$$\langle H\rangle=E_{\rm ph}+E_{\rm MDW} , \quad (13)$$

where $E_{\rm ph}$ is the average energy of phonons with frequencies $E_{l,m}(\vec{q})$ and $E_{\rm MDW}$ is the energy gain due to static displacements of atoms and is given by

$$E_{\rm MDW}=-\sum_{l,m}\sum_{\vec{q}}\frac{|g_{l,m}(\vec{q})|^2}{\hbar E_{l,m}(\vec{q})} . \quad (14)$$

In order to describe the arrangement of the triangular lattice of intercalant layers relative to the adjacent hexagonal lattices of carbon layers, we introduce θ which is defined as an angle between $\vec{G}_{100}$ and $\vec{\tau}_{100}$ in reciprocal-lattice space. Then the most stable orientational arrangement of the two lattices is given by minimizing the total free energy with respect to θ.

To evaluate the free energy $F=\langle H\rangle-TS$ we note that the θ dependence of F is essentially contained in H, where, however, $E_{l,m}(\vec{q})$ is assumed to be not dependent on θ for the temperature range under consideration. In principle, there may be contributions to the entropy term of F from the atomic configurations and from the phonons. Note, however, that for each value of θ there are only two configurations possible corresponding to $+\theta$ and $-\theta$. Therefore, for the case of the homogeneous triangular incommensurate intercalate lattices, the configuration entropy is θ independent. The phonon-entropy contribution is also θ independent because phonon entropy is a function of $E_{l,m}(\vec{q})$.

Until now we have employed the quasiharmonic phonon approximation to establish the free energy. It is obviously desirable to take into account anharmonic effects. However, given the incommensurability of the intercalate lattice with respect to the carbon lattice, a self-consistent solution for $E_{l,m}(\vec{q})$ becomes inaccessible because the dynamical matrix would be of infinite dimension. Therefore, we approximate the anharmonic effects with the following procedure.

We formally follow the self-consistent phonon approximation method.[11] Then we obtain the same expression [Eq. (14)] for E_{MDW} as derived above, provided that $U(\vec{q})$ in Eqs. (6)–(8) is replaced by a potential renormalized by the motion of carbon and intercalant atoms.[11] The renormalization factor would be written as

$$\exp[-\tfrac{1}{2}q^{\alpha}(W_I^{\alpha\beta}+W_G^{\alpha\beta}-2\Lambda_{ij}^{\alpha\beta})q^{\beta}] ,$$

where α,β specify a Cartesian component, $q^{\alpha}W_i^{\alpha\beta}q^{\beta}$ ($i=I$ or G) is a Debye-Waller factor associated with intercalant or graphite layers, respectively, and $q^{\alpha}\Lambda_{ij}^{\alpha\beta}q^{\beta}$ is a similar (but more complicated) factor.[11] On the other hand, the contribution of phonon entropy to the E_{MDW} in the self-consistent phonon approximation can be calculated perturbationally. It is found that the phonon-entropy effect can be involved in the formulation if the $W_I^{\alpha\beta}$ and $W_G^{\alpha\beta}$ if the renormalization factors are appropriately modified. It should be noted that those factors $W_I^{\alpha\beta}$, $W_G^{\alpha\beta}$, and $\Lambda_{ij}^{\alpha\beta}$ include a phonon occupation number so that they are temperature dependent. Those renormalization factors, however, cannot be calculated rigorously. Therefore in the numerical calculation described in the next section, we make an approximation that the renormalization factor is replaced by a phenomenological factor $\exp(-\frac{1}{2}|\vec{q}|^2W)$, where W is a parameter proportional to the average occupation number of phonons.

It has been experimentally observed in the case of CsC_{24} that the rotation angle θ is essentially temperature independent below 165 K, whereas it decreases and finally vanishes when the temperature increases from 165 towards 228 K.[3] Accordingly, in the orientationally ordered state at temperatures $50\leq T\leq 165$ K, which we address here, we simply assume that the phonon frequencies $E_{l,m}(\vec{q})$ are independent of θ as noted above. Consequently, the rotation angle in the rotationally ordered state is determined by the minimum of E_{MDW}. The results of numerical calculation of E_{MDW} will be described in the next section.

III. RESULTS AND DISCUSSION

The basic idea of constructing phonon dispersion curves $E_{l,m}(\vec{q})$ from the virtual phonon scheme refers to the phonon dispersion relations of the stage-1 GIC intercalated with K (or Rb).[10] The phonon dispersion curves of KC_8 calculated within a force-constant model suggest that they are qualitatively equivalent to those constructed by the following procedure: (1) Fold the phonon dispersion curves of pristine graphite into the Brillouin zone (BZ) of KC_8, (2) superimpose dispersion curves of the optical modes associated with vibrations of intercalant atoms relative to those of carbon atoms, and (3) if modes originating from pristine graphite and those from intercalant atoms couple to each other because they have the same polarization, then diagonalize them. The same prescription, however, is not applicable to the stage-2 GIC's because of the incommensurability mentioned before. Therefore we modify the procedure to construct the phonon dispersions $E_{l,m}(\vec{q})$ as follows. First, we determine separately the dispersion curves of virtual phonons associated with vibrations of intercalant atoms and of those associated with carbon atoms. Then, introducing the dynamical coupling between those virtual phonons, we diagonalize the modes to obtain $E_{l,m}(\vec{q})$. This will be demonstrated for the case of CsC_{24} below.

We ignore the modes polarized parallel to the c axis because they have no effect on the orientational rotation under consideration. We focus our attention on phonons with low frequencies because they give the main contribution to the energy E_{MDW} as is seen from Eq. (14). Frequencies of in-plane modes at the point Γ are determined on a linear-chain model in which atoms are arranged in a sequence $A\alpha AA\alpha AA\cdots$. The masses of α and A are taken as being a mass of the Cs atom and a mass equal to 12 times the carbon mass, respectively, to achieve the ideal in-plane stoichiometry of CsC_{24}. The effective force constants are estimated by referring to neutron data.[12,13]

Nontrivial eigenfrequencies are calculated to be $\omega_G(0)=20.4$ cm^{-1} and $\omega_I(0)=32.8$ cm^{-1}, and the corresponding eigenmodes are obtained. The lower-frequency modes are doubly degenerate and correspond to the E_{2g} rigid-layer shear mode of pristine graphite.[14] The higher-frequency modes are doubly degenerate and correspond to out-of-phase vibrations of the Cs atom relative to carbon atoms. Thus we assign those modes with frequencies $\omega_G(0)$ and $\omega_I(0)$ at the point Γ as being virtual phonon modes associated with vibrations of carbon and intercalant atoms, respectively.

On the other hand, we can assume that the acoustic modes are determined by vibrations mostly of graphite because in-plane bondings between carbon atoms are strong enough even in compounds. Since only phonons with low frequencies have significant influence on the MDW's, the frequencies $\omega_{G,l2}(\vec{q})$ of the acoustic modes are well described by a linear

function vq, where v is taken to be a sound velocity of graphite. The in-plane symmetry of pristine graphite has been taken into account by interpolating the sound velocities between $v_{[110]}$ and $v_{[100]}$ by use of sinusoidal functions.

It is noticed that frequencies $\omega_{G,l1}(\vec{q})$ of the E_{2g} rigid-layer modes should approach the acoustic-mode frequencies $\omega_{G,l2}(\vec{q})$ asymptotically for large $|\vec{q}|$. Thus the dispersion curves of $\omega_{G,l1}(\vec{q})$ are calculated by readjusting interlayer force parameters[14] in the case of pristine graphite to reproduce the point Γ frequency $\omega_G(0)=20.4$ cm^{-1} obtained above.

Frequencies $\omega_{I,l}(\vec{q})$ of virtual phonons associated with the motion of intercalant atoms relative to graphite are assumed to be represented by

$$\omega_{I,L}(\vec{q})=\omega_I(\vec{0})+\alpha_L \sin^2\left[\frac{\pi}{2}\frac{q}{q_{\max}}\right], \quad (15)$$

$$\omega_{I,T}(\vec{q})=\omega_I(\vec{0})+\alpha_T \sin^2\left[\frac{\pi}{2}\frac{q}{q_{\max}}\right], \quad (16)$$

where the suffices L and T denote the longitudinal and transverse modes, respectively, and $q_{\max}$ is the value at the boundary of the BZ of the intercalant lattice. The dispersion of $\omega_{I,L}$ and $\omega_{I,T}$ originates mainly from interactions between intercalant atoms. Taking the radial and tangential force constants between Cs atoms to be of the same order of magnitude as those in the case of KC_8 and RbC_8,[10] we obtain $\alpha_L \cong 50$ cm^{-1} and $\alpha_T \cong 30$ cm^{-1}.

It should be noted that the dispersion curves of $\omega_{I,l}(\vec{q})$ cross the curves of $\omega_{G,l1}(\vec{q})$ and/or $\omega_{G,l2}(\vec{q})$ at around $q \cong 0.05 q_{\max}$ and that virtual phonon frequencies $\omega_{G,l1}$ and $\omega_{G,l2}$ at $q \sim q_{\max}$ are more than ten times the frequencies of $\omega_{I,l}(q_{\max})$. Thus the neglect of phonons with $q > q_{\max}$ does not create any serious errors in the result. We take three branches of virtual phonons with the same polarization L and T, respectively, and construct new phonons with frequencies $E_{l,m}(\vec{q})$. The resultant phonon dispersion curves for CsC_{24} are shown in Fig. 1.

The interaction potential between carbon and Cs atoms is taken to consist of a Born-Mayer-type repulsive part and a screened Coulomb interaction. The Fourier transform is written as

$$U(\vec{q})=\frac{8\pi a}{r_0}\left[\frac{1}{(q^2+r_0^{-2})^2}-\frac{r_0 c}{2}\frac{1}{q^2+\lambda^2}\right]. \quad (17)$$

An isotropic screening is assumed for the Coulomb potential, so that the screening factor is given as

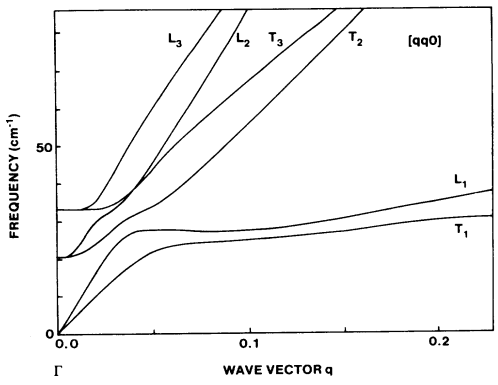

FIG. 1. Phonon dispersion curves for CsC_{24}. The wave vector $\vec{q}$ is measured in units of $4\pi/3d_I$. L and T denote the longitudinal and transverse modes, respectively.

$\lambda=0.067$ Å^{-1} if one assumes that the fraction of charge transfer per Cs is unity. Other parameters are chosen by the conditions that the minimum of the potential $U(r)$ is at $r \cong 3.05$ Å which corresponds to the closest distance yet observed between C and Cs atoms. It also seems reasonable to require $U(\vec{q})$ to have a large value in a certain range of q where the coupling between virtual phonons is considered important. Thus we have chosen $r_0=0.6$ Å, $c=0.063$ Å, and $a=18$ eV.

The MDW energy $E_{\rm MDW}$ for CsC_{24} is calculated by using the phonon dispersion curves shown in Fig. 1, and is plotted against the rotation angle θ in Fig. 2. We find that the minimum of $E_{\rm MDW}$ is at about 14° in good agreement with experiment.[3] In Fig. 2, contributions from each phonon mode are also plotted. It is interesting to observe that the lowest longitudinal mode denoted by L_1 always tends to stabilize the energy at $\theta=19.1°$, which corresponds to the rotation angle of a

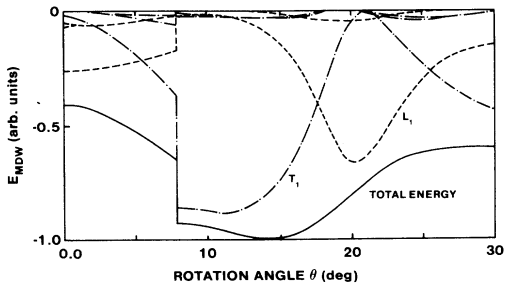

FIG. 2. Plot of $E_{\rm MDW}$ vs θ for CsC_{24}. The value of $E_{\rm MDW}$ is normalized by the absolute value of the minimum of E_{MDW}. The dashed curves are contributions to $E_{\rm MDW}$ from longitudinal modes, whereas dash-dotted curves are those from transverse modes. The discontinuity at $\theta \cong 7°$ is discussed in the text.

$(\sqrt{7}\times\sqrt{7})R\,19.1°$ commensurate superlattice. The lowest-transverse mode denoted by T_1 is, however, more effective in stabilizing the MDW at angles less than 19.1°. This result is associated with a flattening of phonon dispersion curves of the lowest transverse T_1 mode beyond $q/q_{\max}\cong 0.05$ as is seen from Fig. 1. The temperature dependence of E_{MDW} comes from the phonon-entropy term and the factor $\exp(-\frac{1}{2}|\vec{q}|^2 W)$ introduced in the preceding section to take account of anharmonic effects.

The value of W can be estimated by assuming that it is the same order of magnitude as the Debye-Waller factors. Taking the Einstein phonon with a frequency $\omega_I\cong 30\ \mathrm{cm}^{-1}$, the Debye-Waller factor W_I for intercalant layers is estimated to be about 10^{-2} Å^2 for $T\cong 100$ K. On the other hand, the Debye-Waller factor W_G for graphite layers is about 10^{-4} Å^2 if one takes the Debye approximation with $\Theta_D\cong 10^3\ \mathrm{cm}^{-1}$. Thus if we assume that $W\cong W_I$ then we find that W varies in a range of $0.02-0.08$ for $50\lesssim T\lesssim 165$ K. Figure 3 shows the temperature variation of E_{MDW} for several values of W within this temperature range. It is concluded from the numerical calculation that the rotation angle θ is practically independent of temperature in the temperature region under consideration, provided that $E_{l,m}(\vec{q})$ is assumed to be independent of θ. The strong T dependence of θ observed above 165 K for the case of CsC_{24}, therefore, seems to suggest a softening of the T_1 mode.

A similar calculation of the rotation angle has been done for the cases of RbC_{24} and KC_{24}. Parameters involving atomic mass were scaled by a mass ratio from the value of parameters chosen for CsC_{24}. It turns out that the curve E_{MDW} plotted against θ has a minimum at $\theta\cong 12°$ for the case of RbC_{24} ($d_I/d_G=2.45$) and $\theta\cong 8°$ for KC_{24}, respectively. Those values of rotation angle are close to the experimental data[7–9] for RbC_{24} and KC_{24}, respectively, though the experimental results for θ reported by different groups show some variation.

It should be noted here that the discontinuity in E_{MDW} curve at $\theta\cong 7°$ in Fig. 2 is due to the approximation that in the calculation of E_{MDW} we have restricted the wave vectors of phonons to fall within the first BZ of intercalant lattice. Actually, when we rotate the reciprocal lattice of an intercalant layer relative to that of graphite layer, some of the phonon wave vectors satisfying the relation $\vec{q}=\vec{G}-\vec{\tau}$ lie on the boundary of the BZ for $\theta\cong 7°$. Therefore if one restricts the magnitude of the q so as to fall within the BZ, then one has to take phonons with different $\vec{q}$'s depending on $\theta\gtrsim 7°$ or $\theta\lesssim 7°$. It is checked that this restriction for $\vec{q}$'s produces only discontinuities in the E_{MDW} curve and has no significant effect on the rotation angle corresponding to the minimum of E_{MDW}.

So far we have assumed a homogeneous in-plane distribution of intercalant atoms so that the ratio of in-plane lattice constant $Z=d_I/d_G$ is fixed to be 2.44 throughout the crystal. In the case of CsC_{24}, this assumption seems consistent with experimental observations[3] and d_I is 6.02 Å. On the other hand, Clarke *et al.* have recently proposed that the intercalate layer orders into domains bounded by discommensurations.[4] In connection with this point, it seems worthwhile to mention the possibility for the present theory to be extended to the inhomogeneous system. We have checked the case where $Z=d_I/d_G$ is varied. Figure 4 shows the variation of the rotation angle corresponding to the minimum of E_{MDW} as a function of Z. It is interesting to see from Fig. 4 that the rotation angle

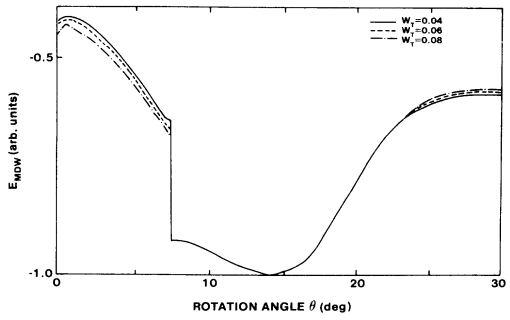

FIG. 3. Temperature dependence of E_{MDW} calculated for CsC_{24} for an appropriate value for the parameter W (see text) which is assumed to be proportional to temperature for $50<T\lesssim 165$ K.

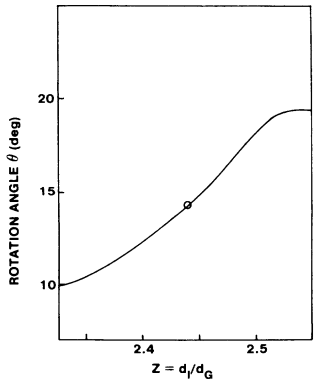

FIG. 4. Variation of the rotation angle for CsC_{24} determined by the minimum of E_{MDW} as a function of $Z=d_I/d_G$. The open circle is the experimental data (Ref. 3).

becomes 19.1° when Z approaches $\sqrt{7}$, so that it exactly corresponds to the $(\sqrt{7}\times\sqrt{7})R$ 19.1° superlattice structure. We have also found that the MDW energy is gained as Z deviates from the ideal value 2.44 that corresponds to the homogeneous in-plane stoichiometry of MC_{24}. Then one might suppose that the intercalant layer structure would consist of a $(\sqrt{7}\times\sqrt{7})R$ 19.1° region and other more dense regions like $(2\times2)R$ 0°, since the average in-plane concentration of intercalant atoms should be kept constant. This is, in fact, consistent with the relation

$$MC_{12\times2}=\tfrac{2}{3}MC_{14\times2}+\tfrac{1}{3}MC_{8\times2}\ , \tag{18}$$

where stoichiometries of $MC_{14\times2}$ and $MC_{8\times2}$ are in correspondence with the commensurate in-plane structures $(\sqrt{7}\times\sqrt{7})R$ 19.1° and $(2\times2)R$ 0°, respectively.

For such a domain structure, however, we have to take into account the locking energy of commensurate domains (commensuration energies) which vanishes in our incommensurate case, and also the significant entropy contribution to free energy associated with configurations of domain walls. Thus, although there is a possibility of having an in-plane domain structure in stage-2 GIC's, further discussion of the domain structure is obviously beyond the scope of the present theory.

IV. SUMMARY AND CONCLUDING REMARKS

The same idea of MDW's as developed by Novaco and McTague[6] in studying the epitaxial ordering of adsorbed films has been extended to study the orientationally ordered state of the stage-2 GIC's; CsC_{24}, RbC_{24}, and KC_{24}. The intercalant atoms are assumed to constitute a homogeneous triangular lattice, so that the arrangement of intercalant lattices is nonregistered with the hexagonal lattice of the adjacent carbon layers.

It is of interest to see that phonons with low frequencies play a crucial role in stabilizing the orientationally ordered state in which the MDW's are generated. The phonon dispersion curves for CsC_{24}, RbC_{24}, and KC_{24} have been calculated by starting from the virtual-phonon scheme. The virtual phonons are originally associated with dynamical motions of intercalant atoms and carbon atoms, respectively, and couple with each other by means of interaction between intercalant and carbon atoms. The resultant phonon dispersion curves for the stage-2 alkali GIC's show a characteristic feature of mixed modes, as demonstrated in Fig. 1. The most stable orientation of intercalant triangular lattice relative to hexagonal graphite lattice is given by the minimum of $E_{\rm MDW}$ as a function of θ, which is defined as an angle between $\vec{\tau}_{100}$ and $\vec{G}_{100}$. It is found that the rotation angle is $\theta=14°$ for CsC_{24}, $\cong12°$ for RbC_{24}, and $\cong8°$ for KC_{24}, respectively, and agrees fairly well with experiments. It should be mentioned that the lowest longitudinal mode L_1 stabilizes the rotation angle at 19.1°, whereas the lowest transverse mode T_1 dominates and tends to depress the rotation angle to values less than 19.1°. Therefore, we conclude that the flattened dispersion curves of low-frequency phonons in the stage-2 GIC's are responsible for the rotation angle observed.

ACKNOWLEDGMENTS

It is a pleasure to acknowledge fruitful discussions with R. Clarke. One of us (C.H.) also acknowledges the hospitality extended to him by the faculty and staff of the Michigan State University Physics Department during his stay there. This research was suppported in part by the NSF under Grant No. DMR-80-10486.

APPENDIX

In this appendix we describe the details of canonical transformation yielding Eq. (9). We also give the equation determining frequencies $E_{l,m}(\vec{q})$ and the explicit expression for $g_{l,m}(\vec{q})$ in Eq. (9). As is noted in the text the longitudinal and transverse virtual-phonon modes of the intercalate atoms are coupled, respectively, with two virtual-phonon modes associated with the carbon atoms with the same polarization direction. In order to diagonalize the Hamiltonian H, therefore, we introduce a linear combination of three virtual-phonon modes with the same polarization for the transverse and longitudinal modes, respectively. Let us define the vectors $\vec{A}_l(\vec{q})$ and $\alpha_l(\vec{q})$ as

$$\begin{aligned}\vec{A}_l(\vec{q})&={}^t\{A_{l1}(\vec{q}),A_{l2}(\vec{q}),A_{l3}(\vec{q}),A_{l1}^{\dagger}(-\vec{q}),A_{l2}^{\dagger}(-q),A_{l3}^{\dagger}(-\vec{q})\}\ ,\\ \vec{\alpha}_l(\vec{q})&={}^t\{a_l(\vec{q}),b_{l1}(\vec{q}),b_{l2}(\vec{q}),a_l^{\dagger}(-\vec{q}),b_{l1}^{\dagger}(-\vec{q}),b_{l2}^{\dagger}(-\vec{q})\}\ ,\end{aligned} \tag{A1}$$

where presuperscript t indicates the transpose of the row vectors, l indicates the polarization direction, and a_l, b_{l1}, and b_{l2} are phonon operators corresponding to the intercalate layer mode, the E_{2g} rigid-layer shear mode, and the acoustic mode of pristine graphite, respectively. The canonical transformation to diagonalize the bilinear terms of H is written in terms of $\vec{A}_l(\vec{q})$ and $\vec{\alpha}_l(\vec{q})$ as

$$\vec{A}_l(\vec{q})=\Gamma_l(\vec{q})\vec{\alpha}_l(\vec{q}) . \tag{A2}$$

Here $\Gamma_l(\vec{q})$ is a 6×6 matrix whose elements are given by (in the following we will omit the wave vector $\vec{q}$ for simplicity of description)

$$\begin{aligned}
&(\Gamma_l)_{i,1}=1/N_{l,i} ,\\
&(\Gamma_l)_{i,2}=-2K_{l,l1}\omega_{I,l}/[\hbar N_{l,i}(\omega_{G,l1}-E_{l,i})(\omega_{I,l}+E_{l,i})] ,\\
&(\Gamma_l)_{i,3}=-2K_{l,l2}\omega_{I,l}/[\hbar N_{l,i}(\omega_{G,l2}-E_{l,i})(\omega_{I,l}+E_{l,i})] ,\\
&(\Gamma_l)_{i,4}=-(\omega_{I,l}-E_{l,i})/[N_{l,i}(\omega_{I,l}+E_{l,i})] ,\\
&(\Gamma_l)_{i,5}=2K_{l,l1}\omega_{I,l}/[\hbar N_{l,i}(\omega_{G,l1}+E_{l,i})(\omega_{I,l}+E_{l,i})] ,\\
&(\Gamma_l)_{i,6}=2K_{l,l2}\omega_{I,l}/[\hbar N_{l,i}(\omega_{G,l2}+E_{l,i})(\omega_{I,l}+E_{l,i})] ,
\end{aligned} \tag{A3}$$

for $1\le i\le 3$, and

$$(\Gamma_l)_{i,j}=\begin{cases}(\Gamma_l)_{i-3,j+3}, & 1\le j\le 3\\ (\Gamma_l)_{i-3,j-3}, & 4\le j\le 6\end{cases}$$

for $4\le i\le 6$ with

$$\begin{aligned}
N_{l,i}=&\frac{4\omega_{I,l}E_{l,i}}{\hbar(\omega_{I,l}+E_{l,i})^2}+\frac{4|K_{l,l1}|^2\omega_{I,l}^2}{\hbar(\omega_{I,l}+E_{l,i})^2}\left[\frac{1}{(\omega_{G,l1}-E_{l,i})^2}-\frac{1}{(\omega_{G,l1}+E_{l,i})^2}\right]\\
&+\frac{4|K_{l,l2}|^2\omega_{I,l}^2}{\hbar^2(\omega_{I,l}+E_{l,i})^2}\left[\frac{1}{(\omega_{G,l2}-E_{l,i})^2}-\frac{1}{(\omega_{G,l2}+E_{l,i})^2}\right] .
\end{aligned} \tag{A4}$$

From commutation relations for $A_{l,m}$ and $A_{l,m}^{\dagger}$ we obtain the equation to determine the frequencies $E_{l,m}$ as

$$\begin{aligned}
&E_{l,m}^6-(\omega_{I,l}^2+\omega_{G,l1}^2+\omega_{G,l2}^2)E_{l,m}^4\\
&\quad+[\omega_{I,l}^2\omega_{G,l1}^2+\omega_{G,l1}^2\omega_{G,l2}^2+\omega_{G,l2}^2\omega_{I,l}^2-4\hbar^2\omega_{I,l}(\omega_{G,l1}|K_{l,l1}|^2+\omega_{G,l2}|K_{l,l2}|^2)]E_{l,m}^2\\
&\quad-(\omega_{I,l}^2\omega_{G,l1}^2\omega_{G,l2}^2-4|K_{l,l1}|^2\omega_{I,l}\omega_{G,l1}\omega_{G,l2}^2-4|K_{l,l2}|^2\omega_{I,l}\omega_{G,l1}^2\omega_{G,l2})=0 .
\end{aligned} \tag{A5}$$

Substitution of Eq. (A2) into Eq. (5) yields, after some manipulation, the expression for the Hamiltonian H written in terms of a new set of operators $\{A_{l,m}(\vec{q}),A_{l,m}^{\dagger}(\vec{q})\}$ as follows:

$$H=\sum_{l=L,T}\sum_{m=1}^{3}\sum_{\vec{q}}\hbar E_{l,m}(\vec{q})[A_{l,m}^{\dagger}(\vec{q})A_{l,m}(\vec{q})+\tfrac{1}{2}]+\sum_{l=L,T}\sum_{\vec{q}}{}^t\vec{A}_l(\vec{q})\Gamma_l^*(\vec{q})\vec{F}_l(\vec{q}) , \tag{A6}$$

where the vector $\vec{F}_l(\vec{q})$ is defined by

$$\vec{F}_l(\vec{q})={}^t(C_{q,l},D_{q,l1},D_{q,l2},C_{q,l},D_{q,l1},D_{q,l2}) . \tag{A7}$$

Comparison of the second term of Eq. (A6) with the second term of Eq. (9) yields the explicit expression for $g_{l,m}(\vec{q})$:

$$\begin{aligned}
g_{l,1}&=[(\Gamma_l)_{1,1}^*+(\Gamma_l)_{1,4}^*]C_{q,l}+[(\Gamma_l)_{1,2}^*+(\Gamma_l)_{1,5}^*]D_{q,l1}+[(\Gamma_l)_{1,3}^*+(\Gamma_l)_{1,6}^*]D_{q,l2} ,\\
g_{l,2}&=[(\Gamma_l)_{2,1}^*+(\Gamma_l)_{2,4}^*]C_{q,l}+[(\Gamma_l)_{2,2}^*+(\Gamma_l)_{2,5}^*]D_{q,l1}+[(\Gamma_l)_{2,3}^*+(\Gamma_l)_{2,6}^*]D_{q,l2} ,\\
g_{l,3}&=[(\Gamma_l)_{3,1}^*+(\Gamma_l)_{3,4}^*]C_{q,l}+[(\Gamma_l)_{3,2}^*+(\Gamma_l)_{3,5}^*]D_{q,l1}+[(\Gamma_l)_{3,3}^*+(\Gamma_l)_{3,6}^*]D_{q,l2} .
\end{aligned} \tag{A8}$$

*Permanent address: Department of Applied Physics, Tohoku University, Sendai, Japan.

[1]S. A. Solin, Adv. Chem. Phys. 49, 455 (1982).

[2]M. S. Dresselhaus and G. Dresselhaus, Adv. Phys. 30, 139 (1981).

[3]R. Clarke, N. Caswell, S. A. Solin, and P. W. Horn, Phys. Rev. Lett. 43, 2018 (1979); Physica (Utrecht) 99B, 457 (1980).

[4]R. Clarke, J. N. Gray, H. Homma, and M. J. Winokur, Phys. Rev. Lett. 47, 1407 (1981).

[5]H. Zabel, *Ordering in Two Dimensions,* edited by S. K. Sinha (North-Holland, Amsterdam, 1981), p. 61.

[6]A. D. Novaco and J. P. McTague, Phys. Rev. Lett. 38, 128 (1977); J. P. McTague and A. D. Novaco, Phys. Rev. B 19, 5299 (1979).

[7]A. N. Berker, N. Kambe, G. Dresselhaus, and M. S. Dresselhaus, Phys. Rev. Lett. 45, 1452 (1980).

[8]Y. Yamada, I. Naiki, T. Watanabe, T. Kiichi, and H. Suematsu, Physica (Utrecht) 105B, 277 (1981).

[9]H. Suematsu, M. Suzuki, H. Ikeda, and Y. Endoh, Synth. Met. 2, 133 (1980).

[10]C. Horie, M. Maeda, and Y. Kuramoto, Physica (Utrecht) 99B, 430 (1980).

[11]A. D. Novaco, Phys. Rev. B 19, 6493 (1979).

[12]W. D. Ellenson, D. Seemingson, D. Guérard, D. G. Onn, and J. E. Fischer, Mater. Sci. Eng. 31, 137 (1977).

[13]H. Zabel and A. Magerel, in Proceedings of the International Conference on Physics of Intercalation, Trieste, 1981.

[14]M. Maeda, Y. Kuramoto, and C. Horie, J. Phys. Soc. Jpn. 47, 337 (1979).